NDT and E International 93 (2018) 18–23

Contents lists available at ScienceDirect

NDT and E International

journal homepage: www.elsevier.com/locate/ndteint

Ultrasonic non-destructive testing of cardboard tubes using air-coupled transducers

Nicolas Quaegebeur [a,*], Patrice Masson [a], Alain Berry [a], Cédric Ardin [b], Pierre-Michel D'Anglade [b]

[a] GAUS, Université de Sherbrooke, Sherbrooke, QC, J1K2R1, Canada
[b] ABZAC Canada, Drummondville, QC, J2B 6Y8, Canada

ARTICLE INFO

Keywords:
Guided waves
Cardboard
Tubes
Air-coupled transducers

ABSTRACT

Cardboard tubes are commonly used for industrial plastic film wrapping due to their low cost, high compression strength, reliability and low sensitivity to environmental changes. In order to guarantee the high radial compression strength during the manufacturing process, destructive testing such as manual peeling or non-destructive testing using acoustic impedance measurements are currently performed on a regular basis. In order to achieve a continuous quality control, automatic and non-contact inspection still need to be developed. In this paper, a method and apparatus for non-contact and rapid inspection of cardboard tubes is presented. The principle is based on the use of capacitive air-coupled transducers at frequencies below 20 kHz for generation and measurement of propagative flexural waves in a pitch-and-catch configuration. Sensitivity analysis is performed for different modes and damage types and is validated experimentally for four flaw types typically observed during the manufacturing process. Experimental validation of detection and flaw quantification is demonstrated using both amplitude and time-of-flight of wave packets at different frequencies, allowing automatic quality control of the manufacturing process.

1. Introduction

Cardboard tubes are commonly used for industrial plastic film wrapping due to their low cost, high compression strength, reliability and low sensitivity to environmental changes. However, since the cardboard tubes are subject to very large compression loads during the wrapping process, a small decrease in strength may lead to dramatic consequences such as the loss of a whole material film roll or machinery damaging. Typical reported damages encountered during the whole manufacturing process include the lack of adhesive, the presence of a liner joint while connecting successive rolls of liner, changes of liner thickness, decrease of laminated surface due to a reduction of liner width, or improper curing process leading to an excessive humidity within the tube.

For this purpose, a refined strategy for quality control of the cardboard tubes is required. Destructive testing is classically conducted at regular intervals, and include manual measurement of thickness, radius and length, or manual peeling of a tube in order to detect delaminations or voids, or radial core crush experiments. The compression limit is thus assessed and compared to reference values in order to reject or accept the whole tube batch. This process is extremely time consuming since a qualified technician is required and is relatively ineffective to reject locally damaged or improperly cured tubes.

Based on these observations, a systematic, rapid and automatic inspection procedure is required and the sensitivity to those different damage types should be demonstrated. For this purpose, the estimation of flexural modulus has been first proposed using three point bending technique [1] or traction tests [2]. Acoustic measurements have also been proposed as an attractive alternative in order to estimate the flexural modulus of a tube based on its first flexural mode resonance frequencies [1,3]. However, since this process requires installing the tube on a standard mounting device, it is also time consuming, such that difficulties may arise for practical implementation in the manufacturing process.

Numerous Non-Destructive Testing (NDT) strategies have been proposed for inspection of paper liner and sheets. Those include contact ultrasound transducers [4,5], photo-acoustic transducers for characterization of bulk [6,7], guided waves [8–11], air-coupled probes for characterization of guided waves propagation [12,13] or using through-the-thickness transmission techniques [14–17]. In all cases, those studies use propagating waves for the mechanical characterization or thickness measurement of paper sheets in static configuration. The extension to the translation movement has been then presented using laser-excitation and measurement techniques [18–22]. To the best of our knowledge, no data

* Corresponding author.
E-mail address: nicolas.quaegebeur@usherbrooke.ca (N. Quaegebeur).

https://doi.org/10.1016/j.ndteint.2017.09.011
Received 2 April 2017; Received in revised form 6 September 2017; Accepted 25 September 2017
Available online 28 September 2017
0963-8695/

are available for cardboard assemblies and multilayer tubes, except using a modal approach that is only sensitive to large scale damages, such as large cracks, holes or excessive humidity [23,24].

In this paper, a method and apparatus for non-contact and rapid inspection of cardboard tubes is presented. The principle is based on the use of capacitive air-coupled transducers at frequencies below 20 kHz for generation and measurement of propagative flexural waves in a pitch-and-catch configuration. The novelty resides in the non-contact generation and measurement of multiple flexural modes for damage detection in small and thick cardboard tubes. Sensitivity analysis is performed for different modes and damage types and is validated experimentally for four flaw types typically observed during the manufacturing process. Experimental validation of detection and flaw quantification is demonstrated using both amplitude and Time-of-Flight (ToF) of wave packets at different frequencies, allowing automatic quality control of the manufacturing process.

Section 2 presents the structure under study and the sensitivity analysis of the flexural waves with respect to geometrical and material changes. Section 3 presents the experimental setup, signal processing steps and results obtained on 50 different tubes subject to various typical flaws.

2. Non-destructive testing using guided waves

2.1. Structure of interest

The structure under study is a cardboard tube of 460 mm length, 81 mm outer diameter and 3.55 mm wall thickness. This structure is composed of an assembly of 10 plies of recycled paper liners of 130 mm width and 0.35 mm thickness that are bonded together using water-based glue, and wrapped using a specific orientation in order to increase the core crush resistance of the assembly [25], as presented in Fig. 1. The assembly is then cut before curing in a controlled environmental chamber during 24 h.

2.2. Guided wave propagation in cardboard tubes

Since all the tubes are to be inspected without slowing down the production line, a rapid and global inspection method has to be proposed. For this purpose, local ultrasound methods for pipes and tubes such as through transmission ultrasound, pulse-echo or phased-array offer local inspection and cannot be retained [26]. Due to their relatively small wavelength, sensitivity to various damage types and ability to travel over large distances, guided waves are proposed here, allowing global inspection of the tube over its whole surface by the use of flexural modes.

Fig. 2 presents the dispersion curves for guided waves propagating in the cardboard tube, i.e. the phase and group velocity of the first modes as a function of frequency. The nomenclature and method used for the calculation of phase and group velocity curves follow the ones proposed in Ref. [27], for which longitudinal modes are denoted by (L), torsional modes by (T) and flexural modes by (F). Two indices are used, corresponding to the radial and thickness mode orders respectively. For the calculation of dispersion curves, the tubes are considered infinitely long and free of external loads. Moreover, the cardboard assembly is assumed isotropic with a mean density of 750 kg/m^3, a Young modulus of 3 GPa and a Poisson's ratio of 0.3 following previous study on similar materials [3].

Due to the large thickness and small diameter of the geometry of interest, a large number of modes is observed in the audible bandwidth, i.e. below 20 kHz. The longitudinal mode $L(0,1)$ and torsional mode $T(0,1)$ corresponding to pure compression and torsion in the length and radial direction, respectively, are presented but not considered in the following study. This can be explained by the difficulty to generate them using non-contact transducers in this frequency range since they are mostly constituted of in-plane motion. Thus, classical damage detection techniques used for pipeline inspection [28] using $L(0,1)$ or $L(0,2)$ modes cannot be used here.

The flexural modes are proposed instead due the ease of generation and measurement using classical contact and non-contact transducer that are mostly sensitive to out-of-plane motion. In the frequency range of interest, i.e. below 20 kHz, the first nine flexural modes $F(n,1)$, where n represents the number of cycles of variation around the circumference, have approximatively the same phase velocity of 450 m/s above 2 kHz, such that mode selectivity is difficult to achieve and multi-mode propagation occurs.

2.3. Damage sensitivity of flexural modes

In order to determine the effect of a potential damage on wave propagation of flexural modes, the variations of phase and group velocities with respect to a reduction of thickness or flexural modulus are described in Fig. 3. In order to be representative, typical decreases of 10% are applied to both parameters as suggested in Ref. [29]. Only the flexural modes $F(n,1)$ with $n<9$ are presented for clarity and the results are expressed in terms of relative changes with respect to the undamaged case. A reduction of 10% of the thickness corresponds to the case of a missing liner that may occur during the manufacturing process. The other damage scenario corresponds to a decrease of Young's modulus that may be due to excessive humidity or a reduction of laminated area.

In the case of thickness reduction, a decrease of 5% of both phase and group velocities is observed above 10 kHz for the $F(1,1)$ mode. In the case of a reduction of Young's modulus, the same overall reduction of phase velocity is observed with a peak around 8 kHz corresponding to a maximal reduction of 12%. The group velocity for this mode exhibits a strong variation in the frequency range of interest with a decrease up to 20% below 8 kHz and an increase of group velocity up to 10% above 8 kHz. In the case of a wall thickness reduction, only a decrease of group velocity up to 10% is observed for this mode. For the higher order modes,

Fig. 1. Description of the cardboard tube geometry used in this study (left). Presentation of the final product wrapped with cellophane (right).

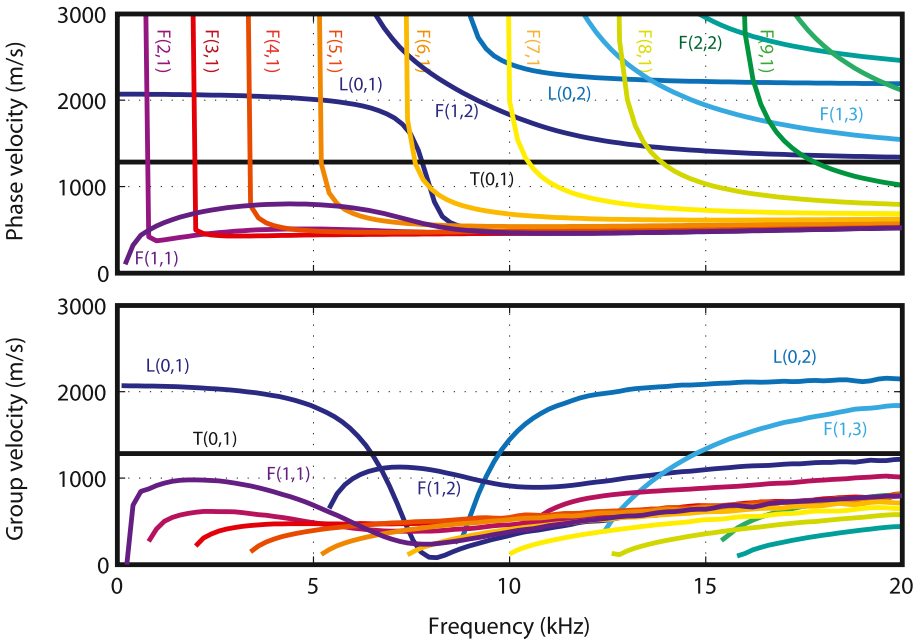

Fig. 2. Phase (top) and group (bottom) velocities for an undamaged tube.

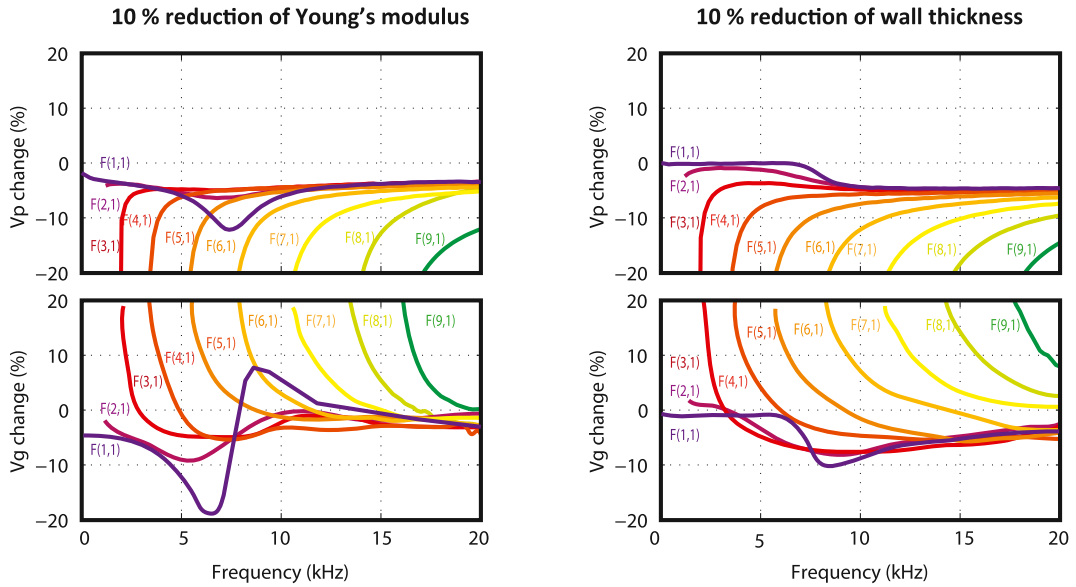

Fig. 3. Phase (top) and group (bottom) velocity changes (in percent) for the various flexural modes in the case of a 10% change of Young modulus (left) or thickness (right).

an overall reduction of phase velocity and increase of group velocity is observed up to 20% close to the cut-off frequencies.

Thus, depending on the damage scenario and severity, changes of group velocity, and thus ToF of the propagating wave-packets are expected. Moreover, the decrease of phase velocity is responsible for a change of acoustic coupling i.e. a change of refraction angle between acoustic and mechanical waves, such that a change of amplitude is expected using air-coupled transducers as described in Ref. [13].

3. Experimental validation

3.1. Strategy for generation and measurement

In order to guarantee rapid inspection of each tube in the production line, non-contact solutions are preferred over classical contact systems such as piezoceramics mounted on angle wedges. Among existing non-contact solutions for generation of guided waves, air-coupled probes or optical solutions are available for both generation and measurement of flexural waves. However, in the frequency range of interest (below 20 kHz), pulsed excitation using Nd:Yag laser would be inefficient, and only air-coupled solutions can be envisioned for a practical implementation [30,31].

Fig. 4 presents the experimental setup in the laboratory environment. Two capacitive broadband air-coupled transducers manufactured at Université de Bordeaux - I2M are located at both ends of the tube with an incidence angle of 38°, corresponding to a phase velocity of 430 m/s. This allows selective generation of all flexural modes $F(n,1)$ in the frequency range of interest, i.e. between 2 and 20 kHz. In order to avoid direct propagation through air, a 50 mm thick porous melamine panel is placed between the two probes.

Measurement of the transfer function between the actuator and the sensor is performed using sub-band excitation [32]. The principle resides

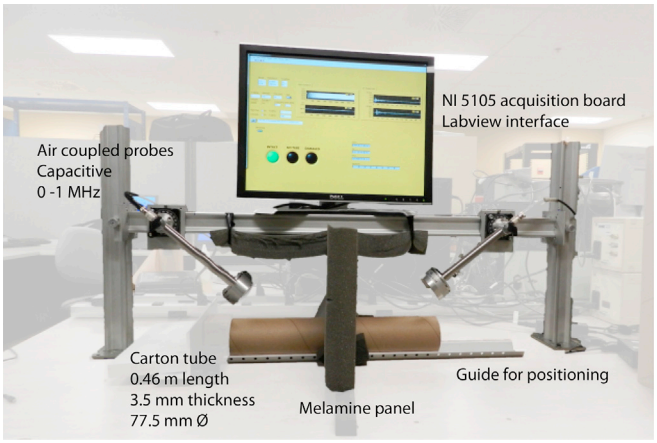

Fig. 4. Experimental setup using air-coupled transducers.

in the use of a sequence of multiple burst signals of limited bandwidth as input in conjunction with appropriate reconstruction filters in order to extract the transfer function of a given system with a high Signal to Noise Ratio (SNR) over a given bandwidth. For this purpose, five sub-bands are used from 5 kHz to 45 kHz by steps of 10 kHz. The input signals are then amplified using a high voltage amplifier (NOVO UA-8200) and measurement is performed by a high impedance acquisition board (National Instrument NI 5105) controlled via a custom LabVIEW interface.

Fig. 5 presents the reconstructed transfer function between the emitter signal and the measured response at the other air-coupled probe in terms of magnitude and phase for ten different undamaged cardboard tubes up to 50 kHz. This transfer function takes into account the propagation in the air gaps between the probes and the tube and the propagation of the guided wave in the tube itself. Since a guide rail is used for positioning, the air gap is assumed constant for all the test, such that the discrepancies between the measured transfer function can be attributed to changes in the propagation of guided waves in the tube. Due to small local variations in the liner material, width or thickness, the repeatability of the measured transfer function is not guaranteed for all the undamaged samples above 25 kHz. Moreover, due to the high material damping, low SNR is observed above 20 kHz. This justifies the choice of the frequency range of interest between 2 and 20 kHz, for which repeatability is ensured within an undamaged batch and SNR above 40 dB is observed.

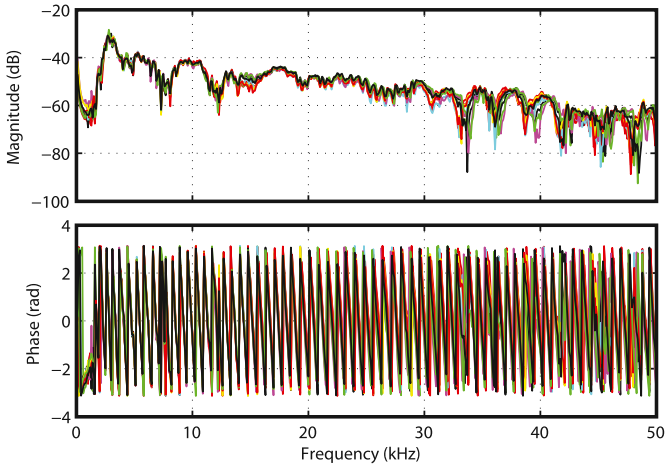

Fig. 5. Transfer functions magnitude (top) and phase (bottom) for ten different undamaged tubes in order to demonstrate the in-group variability.

3.2. Extracted metrics

In order to extract metrics related to the flaw type and severity, narrow-band (burst) reconstruction of the measured signal is performed from the measured transfer functions using inverse Fourier transform as presented in Ref. [33]. This allows interrogation at different frequencies and easy measurement of group velocity through ToF and amplitude of the measured response that is related to material damping but also to changes of phase velocity through a modification of refraction angle between the acoustic and mechanical waves as described in section 2.3 and pointed out in Ref. [13].

For this purpose, 3.5 cycles Hanning bursts at 5 and 10 and 15 kHz are used is order to cover different frequency ranges, and thus different wavelengths from 10.0 mm to 3.3 mm. Fig. 6 presents the reconstructed signals for the undamaged batch of ten different tubes in order to demonstrate the repeatability and complexity of measured signals. The mean group velocities and wavelengths for the propagating flexural modes are also indicated in Fig. 6. At 5 kHz and 10 kHz, multiple mode and dispersive propagation are observed with a distortion of the wave-packet from 3.5 cycles to almost 7 cycles at 10 kHz. Above 15 kHz, the wave dispersion is limited in accordance with the predicted constant group velocity for all the flexural modes as observed in Fig. 2. The extraction of ToF and amplitude at the maximal peak value are then performed using the signal envelope computed using the magnitude of the analytic signal (Hilbert transform).

3.3. Results for typical flaws

In order to demonstrate the repeatability and robustness of the proposed metrics, measurements have been performed on five specifically manufactured batches of ten cardboard tubes each, in order to represent the four typical flaws encountered during the manufacturing process, as described in Table 1. The relative values of radial compression strengths measured over ten different tubes are presented in order to classify the influence on product quality with respect to the flaw type.

The results obtained over the five batches at 5 and 10 kHz are presented in Fig. 7 using the two metrics proposed in the previous section (amplitude and ToF). The results obtained at 15 kHz are not presented here since the sensitivity to the different flaw types is maximal between 5 and 10 kHz as presented in Fig. 3. The frequencies used for damage detection and identification are thus chosen in the audible range (i.e. below 20 kHz). Thus, the process will be audible and also affected by speech and surrounding noise. For this purpose, a confinement area with anechoic conditions should be ensured for practical implantation of the process.

A simple statistical analysis is performed in order to determine the thresholds for flaw detection. In each case, a box plot representation is used, for which the central mark indicates the median, the bottom and top edges of the box indicate the 25th and 75th percentiles respectively. The whiskers extend to the most extreme data points not considered outliers, plotted individually using the + symbol. A color chart is also added based on the metrics obtained for all the tubes in a batch with respect to the extreme values of the undamaged batch (U). For instance, if all the tubes from a batch are identified as flawed, the color chart associated to the metrics of interest is red, while a yellow or green color denote a metrics for which the tubes are partially or not at all identified as flawed.

In Fig. 7, it appears that all the four damage types can be accurately identified by comparing to the undamaged (U) case. For this, a reference group is required in order to define boundary values for the metrics of interest. The liner joint (J) can be detected by looking at the ToF at 5 kHz, while no influence at 10 kHz (and above) is observed. Since this flaw is very local (the liner joint is about 50 mm long and may be localized anywhere in the tube), not all the flexural modes may be sensitive to it. This could explain why the joint can only be detected at 5 kHz.

The change of liner width (W) or humidity (H) are responsible for a

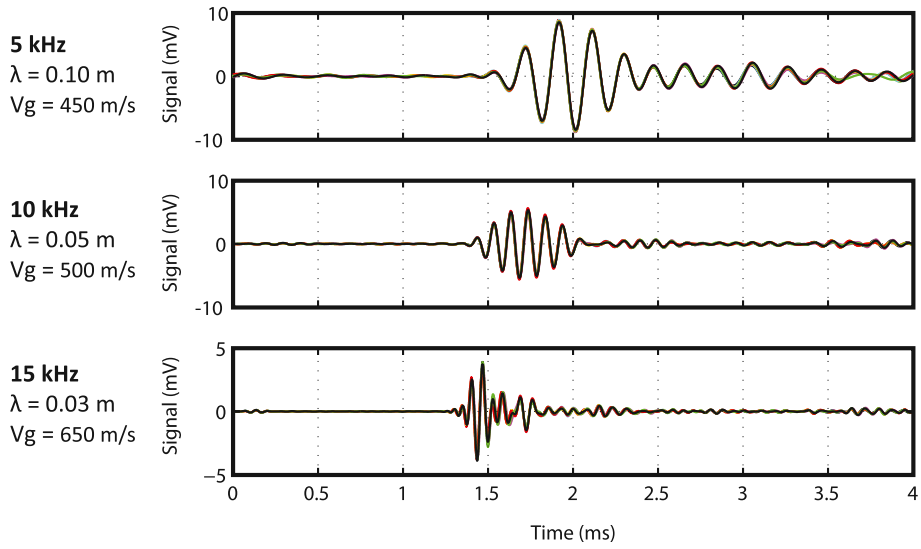

Fig. 6. Reconstructed time-domain signals at the sensor for a 3.5 cycles burst at 5 kHz (top), 10 kHz (middle) and 15 kHz (top). The ten signals obtained on different undamaged tubes are superimposed in order to demonstrate the variability of the measurements.

Table 1
Presentation of the typical flaws and influence on the radial compression.

Name	Description	Relative compression
U	Undamaged - Reference measurements	100%
J	Liner Joint - Presence of an adhesive joint in a liner	97%
W	Liner width - Reduction of 1 mm width for 5 liners	95%
T	Wall thickness - Decrease of 15% of thickness	93%
H	Humidity - Increase of moisture content	47%

decrease in both amplitude and ToF at 10 kHz, such that those two flaw types may have a similar cause. Indeed, the decrease of ToF, meaning an increase of group velocity at 10 kHz may be attributed to a decrease of Young's modulus as suggested in Fig. 3 for the $F(1,1)$ mode. Moreover, the sensitivity can also be predicted by the numerical model and the discrepancies at 5 kHz allows for a discrimination between those two flaw types, since a decrease of ToF at 5 kHz is observed for the (H) batch while a decrease of amplitude is observed for the (W) batch. This might be attributed to the sensitivity of the two flaw types to different flexural modes.

Concerning the thickness decrease (T), an inverse effect is observed with an increase of amplitude and ToF at 10 kHz. The increase of ToF attributed to a decrease of group velocity and the insensitivity at 5 kHz are coherent with the numerical predictions of Fig. 3 for $F(1,1)$ mode.

Thus, with this simple measurement at two different frequencies, it is possible to discriminate between the four flaw types. This relies on the proper definition of thresholds for the undamaged tubes, such that a baseline measurement protocol is required. Since the air and guided wave propagation are sensitive to ambient temperature and humidity, this baseline measurement is required at periodic intervals in order to compensate for environmental changes. However, since the evaluation process can easily be automated, a sliding average process might also be acceptable.

4. Conclusion

This article presents a method and apparatus for non-contact and rapid inspection of cardboard tubes. The principle is based on the use of capacitive air-coupled transducers at frequencies below 20 kHz for generation and measurement of propagative flexural waves. Sensitivity analysis is performed for different modes and damage types and is validated experimentally for four flaw types typically observed during the manufacturing process. Detection of all the damage types is demonstrated using both amplitude and ToF of wave packets at two different frequencies, allowing quality control of the process. Future work include the compensation of environmental changes, the validation of the robustness to acoustic perturbations and automated implementation in the production line.

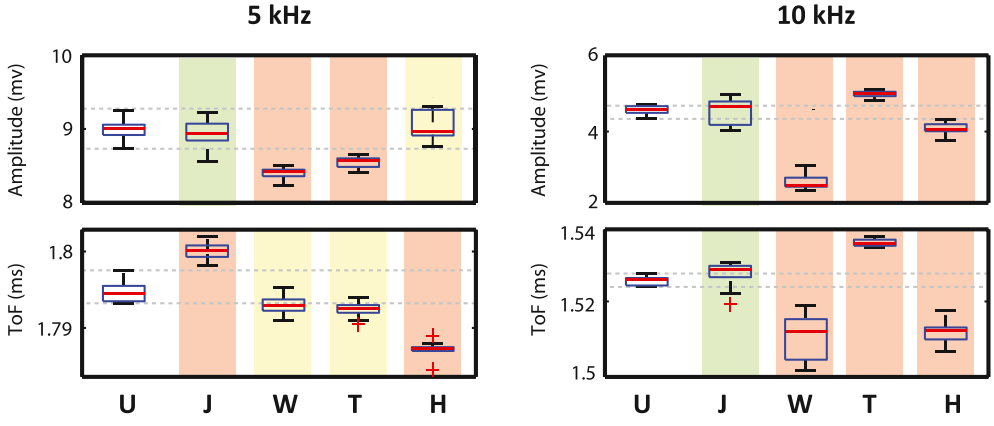

Fig. 7. Results of amplitude (top) and Time-of-Flight (bottom) at 5 kHz (left) and 10 kHz (right) for all the damage types.

Acknowledgements

This work has been conducted with the financial support of the Engineering Research Council of Canada (NSERC) through the ENGAGE grant program number 493300-16.

References

[1] Tech. rep., CCTi Standard Testing Procedure - T 150 Determination of the flexural modulus and bending stiffness of a fiber core by: (A) modal analysis and (B) three point bending. 2008.
[2] Yokoyama T, Nakai K. Evaluation of in-plane orthotropic elastic constants of paper and paperboard. Dimensions 2007;60:50.
[3] Bank L, Gerhardt T, Gordis J. Dynamic mechanical properties of spirally wound paper tubes. J Vib Acoust Stress Reliab Des 1989;111(4):489–90.
[4] Brodeur PH, Hall MS, Esworthy C. Sound dispersion and attenuation in the thickness direction of paper materials. J Acoust Soc Am 1993;94(4):2215–25.
[5] Habeger C, Wink W. Ultrasonic velocity measurements in the thickness direction of paper. J Appl Polym Sci 1986;32(4):4503–40.
[6] Bonnin A, Huchon R, Deschamps M. Ultrasonic waves propagation in absorbing thin plates: application to paper characterization. Ultrasonics 2000;37(8):555–63.
[7] Brodeur PH, Johnson MA, Berthelot YH, Gerhardstein JP. Noncontact laser generation and detection of lamb waves in paper. J Pulp Pap Sci 1997;23(5):J238.
[8] Johnson M, Berthelot Y, Brodeur P, Jacobs L. Investigation of laser generation of lamb waves in copy paper. Ultrasonics 1996;34(7):703–10.
[9] Fällström K-E, Gren P, Mattsson R. Determination of paper stiffness and anisotropy from recorded bending waves in paper subjected to tensile forces. NDT E Int 2002;35(7):465–72.
[10] A. Blouin, B. Reid, J.-P. Monchalin, Laser-ultrasonic measurement of elastic properties of a thin sheet and of tension applied thereon, US Patent 6,543,288 (Apr. 8 2003).
[11] Zhang X, Jackson T, Lafond E. Stiffness properties and stiffness orientation distributions for various paper grades by non-contact laser ultrasonics. NDT E Int 2006;39(7):594–601.
[12] Álvarez-Arenas TG, Soto D. Characterization of mineral paper by air-coupled ultrasonic spectroscopy. Ultrasonics 2012;52(6):794–801.
[13] K. Itsumi, T. Yamamoto, T. Nakano, S. Ikari, J. Miura, T. Saito, T. Nishimura, Stiffness detector, stiffness detection method, and paper sheet processor including stiffness detector, US Patent 8,156,808 (April 2012).
[14] Gómez TE, González B, Montero F. Paper characterization by measurement of thickness and plate resonances using air-coupled ultrasound. In: Ultrasonics symposium, vol. 1. IEEE; 2002. p. 865–8.
[15] Khoury M, Tourtollet GE, Schröder A. Contactless measurement of the elastic young's modulus of paper by an ultrasonic technique. Ultrasonics 1999;37(2):133–9.
[16] McIntyre CS, Hutchins DA, Billson DR, Stor-Pellinen J. The use of air-coupled ultrasound to test paper. IEEE Trans Ultrason Ferroelectr Freq Control 2001;48(3):717–27.
[17] Stor-Pellinen J, Hæggström E, Luukkala M. Measurement of paper-wetting processes by ultrasound transmission. Meas Sci Technol 2000;11(4):406.
[18] Jong JH, Brodeur PH, Lafond E, Gerhardstein JP, Pufahl BM. Laser ultrasonics for noncontact measurement of lamb waves in static and moving paper. J Pulp Pap Sci 2000;26(10):358–66.
[19] Kažys R, Stolpe P. Ultrasonic non-destructive on-line estimation of the tensile stiffness of a running paper web. NDT E Int 2001;34(4):259–67.
[20] Ridgway P, Hunt A, Quinby-Hunt M, Russo R. Laser ultrasonics on moving paper. Ultrasonics 1999;37(6):395–403.
[21] Ridgway P, Russo R, Lafond E, Habeger C, Jackson T. Laser ultrasonic system for online measurement of elastic properties of paper. J Pulp Pap Sci 2003;29(9):287–91.
[22] Walter JB, Telschow KL, Gerhardstein J, Pufahl B, Habeger C, Lafond E, et al. Fabry-perot laser ultrasonic elastic anisotropy measurements on a moving paper web. In: AIP conference proceedings, vol. 509; 2000. p. 247–54.
[23] A. Dabkevičius, N. Nagineviˇciutė, E. Kibirkštis, Non-destructive identification of vibrations of cardboard boxes., Journal of Vibroengineering 13(4).
[24] E. Kibirkštis, A. Kabelkaite, A. Dabkevièius, L. Ragulskis, Investigation of vibrations of packaging materials., Journal of Vibroengineering 10(2).
[25] G. Biagiotti, Machine for producing cardboard or similar tubes, with means for cutting the tube into sections of predetermined lengths, US Patent 5,873,806 (Feb. 23 1999).
[26] Tech. rep., ASTM E213–E214e1 A. International, Standard practice for ultrasonic testing of metal pipe and tubing. 2014.
[27] Silk M, Bainton K. The propagation in metal tubing of ultrasonic wave modes equivalent to lamb waves. Ultrasonics 1979;17(1):11–9.
[28] Lowe MJ, Alleyne DN, Cawley P. Defect detection in pipes using guided waves. Ultrasonics 1998;36(1–5):147–54.
[29] Quaegebeur N, Micheau P, Masson P, Castaings M. Methodology for optimal configuration in structural health monitoring of composite bonded joints. Smart Mater Struct 2012;21(10):105001.
[30] Chimenti D. Review of air-coupled ultrasonic materials characterization. Ultrasonics 2014;54(7):1804–16.
[31] Buckley J. Air-coupled ultrasound–a millennial review. In: 15 th world conference on NDT, Rome; 2000.
[32] N. Quaegebeur, P. Masson, P. Micheau, N. Mrad, Broadband generation of ultrasonic guided waves using piezoceramics and sub-band decomposition, IEEE Transactions on Ultrasonics, Ferroelectrics, and Frequency Control 59(5).
[33] Michaels JE, Lee SJ, Croxford AJ, Wilcox PD. Chirp excitation of ultrasonic guided waves. Ultrasonics 2013;53(1):265–70. https://doi.org/10.1016/j.ultras.2012.06.010. http://www.sciencedirect.com/science/article/pii/S0041624X12001333.